Journal of Solid Mechanics Vol. 6, No. 4 (2014) pp. 334-346

Nonlocal DQM for Large Amplitude Vibration of Annular Boron Nitride Sheets on Nonlinear Elastic Medium

A. Ghorbanpour Arani [1,2,*], R. Kolahchi[1], S.M.R. Allahyari[1]

[1]*Faculty of Mechanical Engineering, University of Kashan, Kashan , Islamic Republic of Iran*
[2]*Institute of Nanoscience & Nanotechnology, University of Kashan, Kashan, Islamic Republic of Iran*

Received 2 June 2014; accepted 4 August 2014

ABSTRACT

One of the most promising materials in nanotechnology such as sensors, actuators and resonators is annular Boron Nitride sheets (ABNSs) due to excelled electro-thermo-mechanical properties. In this study, however, differential quadrature method (DQM) and nonlocal piezoelasticity theory are used to investigate the nonlinear vibration response of embedded single-layered annular Boron Nitride sheets (SLABNSs). The interactions between the SLABNSs and its surrounding elastic medium are simulated by nonlinear Pasternak foundation. A detailed parametric study is conducted to elucidate the influences of the nonlocal parameter, elastic medium, temperature change and maximum amplitude on the nonlinear frequency of the SLABNSs. Results indicate that with increasing nonlocal parameter, the frequency of the coupled system becomes lower. The results are in good agreement with the previous researches.

Keywords: Nonlinear vibration; SLABNS; DQM; Nonlocal piezoelasticity theory; Nonlinear elastic medium.

1 INTRODUCTION

IN recent years, a significant amount of research has been focused on nanostructured materials because of their interesting mechanical and physical properties. Carbon nanotubes (CNTs) have shown great potential for technological applications. It is well established that CNTs possess exceptional mechanical properties such as high strength to weight and stiffness to weight ratios, and enormous electrical conductivity [1]. However, their applications are limited in high strength and uniform electronic structures. This may be explained by the fact that the electrical properties of CNTs are unstable and range from metallic to semiconducting depending upon the radius and chirality of the tubes [2].

Boron nitride (BN) nanotubes, unlike CNTs, are all semiconductors with a constant wide band gap of 5.5 eV, when their diameter is greater than 9.5˚A. Also, small BN nanotubes show interesting size-dependent electronic and magnetic properties [3]. In the 1960s, Boron nitride sheets and relative structures in hexagonal state (h-BN) have been studied experimentally. It has been found that BN exists in several forms: fibers, nanomesh, nanotubes and nanosheets. Different types of BN include armchair, zigzag and chairal. BN nanostructures exhibit electrically insulated properties, strong chemical and thermal stability but, at the same time, excellent thermal conductivities and mass sensing capabilities [4]. These properties of BNs make them promising candidate materials in a large variety of nanosized electronic and photonic devices such as sensors, actuators and resonators. Furthermore, BNs can be used

* Corresponding author. Tel.: +98 31 55912450; Fax: +98 31 55912424.
E-mail address: aghorban@kashanu.ac.ir (A. Ghorbanpour Arani).

for reinforcement in composite structures due to their high thermal conductivity, high resistance to oxidation at elevated temperatures, and outstanding mechanical properties [4].

Conducting experiments with nanoscale size specimens is found to be difficult and expensive. Therefore, development of appropriate mathematical models for nanostructures is an important issue concerning application of nano-structures. Vibration of nanostructures is of great importance in nanotechnology. Understanding vibration behavior of nanostructures is the key step for many NEMS devices like oscillators, clocks and sensor devices.

Behfar and Naghdabadi [5] studied the nanoscale vibrational analysis of a multi-layered graphene sheets (MLGS) embedded in an elastic medium. Liew [6] proposed a continuum-based plate model to investigate the vibration behavior of MLGSs that are embedded in an elastic matrix. Pradhan [7] presented analytical solutions for vibration of the nanoplates such as graphene sheets. They employed nonlocal theories to bring out the effect of the nonlocal parameter on natural frequencies of the nanoplates. Shen [8] presented nonlinear vibration behavior for a simply supported, rectangular, single layer grapheme sheet (SLGS) in thermal environments. Ansari [9] developed a nonlocal plate model which accounts for the small scale effects to study the vibrational characteristics of MLGSs with different boundary conditions embedded in an elastic medium. On the basis of the constitutive equations of nonlocal elasticity, the Mindlin type equations of motion coupled together through the van der Waals interaction are derived. Pradhan [10] studied the small scale effect on the vibration analysis of orthotropic SLGSs embedded in elastic medium using nonlocal elasticity theory and DQM. Transverse nonlinear vibration of orthotropic double-layered grapheme sheets (DLGSs) embedded in a nonlinear elastic medium under thermal gradient was studied by Ghorbanpour Arani et al. [11], using nonlocal elasticity orthotropic plate theory and DQM. Mohammadi et al. [12] studied the free vibration behavior of circular and annular graphene sheets using the nonlocal elasticity theory based on Bessel functions and new version of DQM.

All of the aforementioned researches are related to non-smart material structures. Salehi-Khojin and Jalili [13] derived the equation of motion for BN nanotubes-based composites subjected to combined electro-thermo-mechanical loadings using three-dimensional equilibrium equations. Based on nonlocal piezoelasticity theory, transverse vibration and instability of embedded double-walled boron nitride nanotubes (DWBNNTs) conveying viscose fluid was studied by Khodami Maraghi et al. [14] using DQM. They showed that the electric field effect on the frequency is approximately constant, while it decreases with increasing temperature change. Electro-thermo-mechanical nonlocal wave propagation analysis of embedded DWBNNTs conveying fluid was presented by Ghorbanpour et al [15] via strain gradient theory. Also, Ghorbanpour et al. [16] applied DQM and nonlocal piezoelasticity theory for electro-thermal vibration of fluid-conveying DWBNNTs embedded in an elastic medium using cylindrical shell theory.

However, to date, no report has been found in the literature on vibration analysis of annular ABNSs. Motivated by these considerations, in order to improve optimum design of smart nanostructures, we aim to investigate the nonlinear nonlocal vibration analysis of SLABNSs embedded in a nonlinear elastic medium using DQM. The influences of nonlocal parameter, aspect ratio, elastic medium coefficients on the frequency of the coupled system are taken into account.

2 BASIC EQUATIONS

A schematic of SLABNS resting on a Pasternak foundation is shown in Fig. 1. The geometrical parameters of the SLABNS are inner radius a , outer radius b and thickness h . The elastic medium containing spring constants of Winkler-type (K_{1w}, K_{2w}) and shear constants of Pasternak-type (G_P).

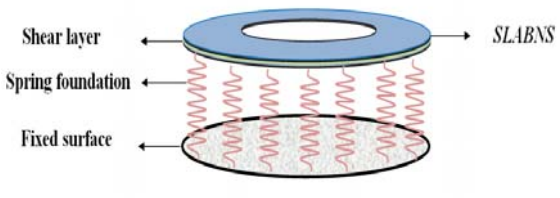

Fig. 1
A schematic of SLABNS resting on a Pasternak foundation.

2.1 Nonlocal piezoelasticity theory

Based on the theory of nonlocal piezoelasticity, the stress tensor and the electric displacement at a reference point depend not only on the strain components and electric-field components at the same position but also on all other points of the body. The nonlocal constitutive behavior for the piezoelectric material can be given as follows [17, 18]

$$\sigma_{ij}^{nl}(x) = \int_v \alpha(|x-x'|,\tau)\sigma_{ij}^{l} dV(x'), \qquad \forall x \in V \tag{1}$$

$$D_k^{nl} = \int_v \alpha(|x-x'|,\tau) D_k^{l} dV(x'), \qquad \forall x \in V \tag{2}$$

where σ_{ij}^{nl} and σ_{ij}^{l} are, respectively, the nonlocal stress tensor and local stress tensor, D_k^{nl} and D_k^{l} are the components of the nonlocal and local electric displacement. $\alpha(|x-x'|,\tau)$ is the nonlocal modulus. $|x-x'|$ is the Euclidean distance, and $\tau = e_0 a / l$ is defined that l is the external characteristic length, e_0 denotes a constant appropriate to each material, and a is an internal characteristic length of the material. Consequently, $e_0 a$ is a constant parameter which is obtained with molecular dynamics, experimental results, experimental studies and molecular structure mechanics. The constitutive equation of the nonlocal elasticity can be written as [18]

$$(1-\mu\nabla^2)\sigma_{ij}^{nl} = \sigma_{ij}^{l}, \tag{3}$$

where the parameter $\mu = (e_0 a)^2$ denotes the small scale effect on the response of structures in nanosize, and ∇^2 is the Laplacian operator in the above equation. Similarly, Eq. (2) can be written to as:

$$(1-\mu\nabla^2)D_k^{nl} = D_k^{l}, \tag{4}$$

2.2 Motion equations

Based on the classical plate theory (CPT) which satisfy Kirchhoff assumption, displacement field is represented as [19]

$$u_r(r,\theta,z,t) = u_0(r,\theta,t) - z\frac{\partial w_0}{\partial r}, \tag{5}$$

$$u_\theta(r,\theta,z,t) = v_0(r,\theta,t) - z\left(\frac{1}{r}\frac{\partial w_0}{\partial \theta}\right), \tag{6}$$

$$u_z(r,\theta,z,t) = w_0(r,\theta,t), \tag{7}$$

where (u_r, u_θ, u_z) denote the total displacements of a point along radial (r), circumferential (θ) and axial (z) directions and (u_0, v_0, w_0) are the displacements of the same points on the mid-plane. Using Eqs. (5)-(7), the nonlinear mechanical strains can be written in term of displacements as:

$$\varepsilon_{rr} = \frac{\partial u_0(r,\theta,t)}{\partial r} + \frac{1}{2}\left(\frac{\partial w_0(r,\theta,t)}{\partial r}\right)^2 - z\frac{\partial^2\left(w_0(r,\theta,t)\right)}{\partial r^2}, \tag{8}$$

$$\varepsilon_{\theta\theta} = \frac{u_0}{r} + \frac{1}{r}\frac{\partial v_0(r,\theta,t)}{\partial \theta} + \frac{1}{r^2}\left(\frac{\partial w_0(r,\theta,t)}{\partial \theta}\right)^2 - \frac{z}{r}\left(\frac{\partial w_0(r,\theta,t)}{\partial r} + \frac{1}{r}\frac{\partial^2\left(w_0(r,\theta,t)\right)}{\partial \theta^2}\right), \tag{9}$$

$$2\varepsilon_{r\theta}=\frac{1}{r}\frac{\partial u_0(r,\theta,t)}{\partial\theta}+\frac{\partial v_0(r,\theta,t)}{\partial r}-\frac{v_0(r,\theta,t)}{r}-\frac{2z}{r}\left(\frac{\partial^2\left(w_0(r,\theta,t)\right)}{\partial r\partial\theta}-\frac{1}{r}\frac{\partial w_0(r,\theta,t)}{\partial\theta}\right). \tag{10}$$

Constitutive equations for SLABNSs can be expressed as follows [15]

$$[\sigma]=[C][\varepsilon]-[h]^T[E], \tag{11}$$

$$[D]=[h][\varepsilon]+[\in][E], \tag{12}$$

where $[\sigma],[\varepsilon],[D]$ and $[E]$ are classical stress, strain, electric displacement and electric field tensors, respectively. Also, $[C],[h]$ and $[\in]$ denote elastic stiffness, piezoelectric and dielectric coefficients matrix, respectively.

Considering radial polarization for SLABNS and using Eqs. (5)-(7), the above equations can be rewritten as:

$$\left(1-\mu\nabla^2\right)\begin{bmatrix}\sigma_r\\ \sigma_\theta\\ \sigma_{r\theta}\end{bmatrix}=\begin{bmatrix}\frac{E}{1-\upsilon^2} & \frac{E\upsilon}{1-\upsilon^2} & 0\\ \frac{E\upsilon}{1-\upsilon^2} & \frac{E}{1-\upsilon^2} & 0\\ 0 & 0 & \frac{E}{2(1+\upsilon)}\end{bmatrix}\begin{bmatrix}\varepsilon_{rr}-\alpha_r\Delta T\\ \varepsilon_{\theta\theta}-\alpha_\theta\Delta T\\ \varepsilon_{r\theta}\end{bmatrix}-\begin{bmatrix}h_{11}\\ 0\\ 0\end{bmatrix}[E_r], \tag{13}$$

$$\left(1-\mu\nabla^2\right)D_r=\begin{bmatrix}h_{11} & 0 & 0\end{bmatrix}\begin{bmatrix}\varepsilon_{rr}-\alpha_r\Delta T\\ \varepsilon_{\theta\theta}-\alpha_\theta\Delta T\\ \varepsilon_{r\theta}\end{bmatrix}+[\in_{11}][E_r], \tag{14}$$

where E,υ,α_r and α_θ are Young's modulus, Poisson's ratio, radial thermal expansion coefficient and circumferential thermal expansion coefficient, respectively. Also E_r in term of electric potential (φ) is given as follow

$$E_r=-\frac{\partial\varphi}{\partial r}. \tag{15}$$

The total electrostatic (U) and kinetic (K) energies of the SLABNS can be expressed as:

$$U=\frac{1}{2}\int\left(\sigma_{rr}\varepsilon_{rr}+\sigma_{\theta\theta}\varepsilon_{\theta\theta}+\sigma_{r\theta}\gamma_{r\theta}-D_rE_r\right)dV, \tag{16}$$

$$K=\frac{1}{2}\int\rho_{BN}\left[\left(\frac{\partial u_r}{\partial t}\right)^2+\left(\frac{\partial u_\theta}{\partial t}\right)^2+\left(\frac{\partial u_z}{\partial t}\right)^2\right]dV, \tag{17}$$

where ρ_{BN} is density of SLABNS. The external work (W) due to surrounding elastic medium is given as:

$$W=\int_0^L\left(-K_{1w}w_0-K_{2w}w_0^3+G_p\nabla^2w_0\right)w_0dx, \tag{18}$$

where K_{1w}, K_{2w} and G_p are respectively, linear Winkler coefficient, nonlinear Winkler coefficient and Pasternak coefficient. The motion equations of embedded SLABNS can be derived by Hamilton's principles as follows

$$\int \left(\delta K - \delta U + \delta W\right) dt = 0. \tag{19}$$

Substituting Eqs. (16)-(18) into Eq. (19), the following motion equations can be derived

$$\delta u : \frac{1}{r}\left[\frac{\partial\left(rN_{rr}\right)}{\partial r} - N_{\theta\theta} + \frac{\partial N_{r\theta}}{\partial \theta}\right] = I_0 \frac{\partial^2 u_0}{\partial t^2}, \tag{20}$$

$$\delta v : \frac{1}{r}\left[\frac{\partial N_{\theta\theta}}{\partial \theta} + \frac{\partial\left(rN_{r\theta}\right)}{\partial r} + N_{r\theta}\right] = I_0 \frac{\partial^2 v_0}{\partial t^2}, \tag{21}$$

$$\begin{aligned}\delta w : &\frac{1}{r}\left[\frac{\partial}{\partial r}\left(rN_{rr}\frac{\partial w_0}{\partial r}\right) + \frac{1}{r}\frac{\partial}{\partial \theta}\left(N_{\theta\theta}\frac{\partial w_0}{\partial \theta}\right) + \frac{\partial^2\left(rM_{rr}\right)}{\partial r^2} - \frac{\partial M_{\theta\theta}}{\partial r} + \frac{1}{r}\frac{\partial^2 M_{\theta\theta}}{\partial \theta^2} + 2\frac{\partial^2 M_{r\theta}}{\partial r \partial \theta} + \frac{2}{r}\frac{\partial M_{r\theta}}{\partial \theta}\right] \\ &-K_{1w}w_0 - K_{2w}w_0^3 + G_p\nabla^2 w_0 = I_0\frac{\partial^2 w_0}{\partial t^2} - I_2\frac{\partial^2}{\partial t^2}\left(\frac{1}{r}\frac{\partial}{\partial r}\left(r\frac{\partial w_0}{\partial r}\right) + \frac{1}{r^2}\frac{\partial^2 w_0}{\partial \theta^2}\right),\end{aligned} \tag{22}$$

$$\delta\varphi : \int_{\frac{-h}{2}}^{\frac{h}{2}} \frac{\partial(D_r)}{\partial r} dz = 0, \tag{23}$$

where the force resultants $(N_{rr}, N_{\theta\theta}, N_{r\theta})$ and the moment resultants $(M_{rr}, M_{\theta\theta}, M_{r\theta})$ can be defined as:

$$\begin{Bmatrix} N_{rr} \\ N_{\theta\theta} \\ N_{r\theta} \end{Bmatrix} = \int_{\frac{-h}{2}}^{\frac{h}{2}} \begin{Bmatrix} \sigma_{rr} \\ \sigma_{\theta\theta} \\ \sigma_{r\theta} \end{Bmatrix} dz, \tag{24}$$

$$\begin{Bmatrix} M_{rr} \\ M_{\theta\theta} \\ M_{r\theta} \end{Bmatrix} = \int_{\frac{-h}{2}}^{\frac{h}{2}} \begin{Bmatrix} \sigma_{rr} \\ \sigma_{\theta\theta} \\ \sigma_{r\theta} \end{Bmatrix} z dz. \tag{25}$$

Furthermore, (I_0, I_2) are the mass moments of inertia which can be represented as:

$$I_0 = \int_{\frac{-h}{2}}^{\frac{h}{2}} \rho_{BN} dz, \tag{26}$$

$$I_2 = \int_{\frac{-h}{2}}^{\frac{h}{2}} z^2 \rho_{BN} dz. \tag{27}$$

Using the nonlocal piezoelasticity theory and Eq. (13), the nonlocal stress resultant can be rewritten as:

$$\begin{aligned}\left(1-\mu\nabla^2\right)N_{rr} &= k_{11}\left(\frac{\partial u_0}{\partial r} + \frac{1}{2}\left(\frac{\partial w_0}{\partial r}\right)^2\right) + k_{12}\left(\frac{u_0}{r} + \frac{1}{r}\frac{\partial v_0}{\partial \theta} + \frac{1}{2}\left(\frac{1}{r}\frac{\partial w_0}{\partial \theta}\right)\right) - \left(k_{11}\alpha_r + k_{12}\alpha_\theta\right)\Delta T - hh_{11}\frac{\partial \varphi}{\partial r}, \\ \left(1-\mu\nabla^2\right)N_{\theta\theta} &= k_{12}\left(\frac{\partial u_0}{\partial r} + \frac{1}{2}\left(\frac{\partial w_0}{\partial r}\right)^2\right) + k_{22}\left(\frac{u_0}{r} + \frac{1}{r}\frac{\partial v_0}{\partial \theta} + \frac{1}{2}\left(\frac{1}{r}\frac{\partial w_0}{\partial \theta}\right)\right) - \left(k_{12}\alpha_r + k_{22}\alpha_\theta\right)\Delta T, \\ \left(1-\mu\nabla^2\right)N_{x\theta} &= k_{66}\left(\frac{\partial u_0}{r\partial \theta} + \frac{\partial v_0}{\partial r} - \frac{v_0}{r}\right),\end{aligned} \tag{28}$$

$$\begin{aligned}
\left(1-\mu\nabla^2\right)M_{rr} &= -D\left(\frac{\partial^2 w_0}{\partial r^2}\right)-D\upsilon\left(\frac{1}{r}\frac{\partial w_0}{\partial r}+\frac{1}{r^2}\frac{\partial^2 w_0}{\partial r^2}\right),\\
\left(1-\mu\nabla^2\right)M_{\theta\theta} &= -D\left(\frac{\partial^2 w_0}{\partial r^2}\right)-D\left(\frac{1}{r}\frac{\partial w_0}{\partial r}+\frac{1}{r^2}\frac{\partial^2 w_0}{\partial r^2}\right),\\
\left(1-\mu\nabla^2\right)M_{x\theta} &= -(1-\upsilon)D\left(\frac{1}{r}\frac{\partial^2 w_0}{\partial r\partial\theta}-\frac{1}{r^2}\frac{\partial w_0}{\partial\theta}\right),
\end{aligned} \tag{29}$$

where

$$k_{11}=k_{22}=\frac{Eh}{1-\upsilon^2}, k_{12}=k_{21}=\frac{\upsilon Eh}{1-\upsilon^2}, k_{66}=Gh, \tag{30}$$

$$D=\frac{Eh^3}{12(1-\upsilon^2)}, \textit{flexturalri gidity} \tag{31}$$

where G is shear modulus. Finally, substituting Eqs. (28) and (29) into Eqs. (20)-(23), yields

$$\begin{aligned}
&\frac{1}{r}\left[k_{11}\left(\frac{\partial u}{\partial r}+\frac{1}{2}\left(\frac{\partial w}{\partial r}\right)^2\right)+k_{12}\left(\frac{u}{r}+\frac{1}{r}\frac{\partial v}{\partial\theta}+\frac{1}{r^2}\left(\frac{\partial w}{\partial\theta}\right)^2\right)+hh_{11}\frac{\partial\varphi}{\partial r}\right]+k_{11}\left(\frac{\partial^2 u}{\partial r^2}+\frac{\partial w}{\partial r}\frac{\partial^2 w}{\partial r^2}\right)+\\
&k_{12}\left(\frac{1}{r}\frac{\partial u}{\partial r}-\frac{u}{r^2}-\frac{1}{r^2}\frac{\partial v}{\partial\theta}+\frac{1}{r}\frac{\partial^2 v}{\partial r\partial\theta}-\frac{2}{r^3}\left(\frac{\partial w}{\partial\theta}\right)^2+\frac{2}{r^2}\frac{\partial^2 w}{\partial r\partial\theta}\frac{\partial w}{\partial\theta}\right)-\frac{1}{r^2}\left(k_{12}\left(\frac{\partial u}{\partial r}+\frac{1}{2}\left(\frac{\partial w}{\partial r}\right)^2\right)\right),\\
&+k_{22}\left(\frac{u}{r}+\frac{1}{r}\frac{\partial v}{\partial\theta}+\frac{1}{r^2}\left(\frac{\partial w}{\partial\theta}\right)^2\right)+\frac{1}{r}\left(k_{66}\left(\frac{1}{r}\frac{\partial^2 u}{\partial\theta^2}+\frac{\partial^2 v}{\partial\theta\partial r}-\frac{1}{r}\frac{\partial v}{\partial\theta}\right)\right)+hh_{11}\frac{\partial^2\varphi}{\partial r^2}=I_0\frac{\partial^2 u}{\partial t^2}
\end{aligned} \tag{32}$$

$$\begin{aligned}
&\frac{1}{r}\left[k_{12}\left(\frac{\partial^2 u}{\partial r\partial\theta}+\frac{\partial^2 w}{\partial\theta\partial r}\frac{\partial w}{\partial r}\right)+k_{22}\left(\frac{1}{r}\frac{\partial u}{\partial\theta}+\frac{1}{r}\frac{\partial^2 v}{\partial\theta^2}+\frac{2}{r}\frac{\partial^2 w}{\partial\theta^2}\frac{\partial w}{\partial\theta}\right)+2k_{66}\left(\frac{1}{r}\frac{\partial u}{\partial\theta}+\frac{\partial v}{\partial r}-\frac{v}{r}\right)\right]+\\
&+k_{66}\left(-\frac{1}{r^2}\frac{\partial u}{\partial\theta}+\frac{1}{r}\frac{\partial^2 u}{\partial r\partial\theta}+\frac{\partial^2 v}{\partial r^2}+\frac{v}{r^2}-\frac{1}{r}\frac{\partial v}{\partial r}\right)=I_0\frac{\partial^2 v}{\partial t^2}
\end{aligned}, \tag{33}$$

$$\begin{aligned}
&-D\frac{\partial^4 w}{\partial r^4}-\frac{D}{r^4}\frac{\partial^4 w}{\partial\theta^4}-\frac{D}{r}(1-\upsilon)\frac{\partial^3 w}{\partial r^4}-\frac{D}{r^3}(1+2\upsilon)\frac{\partial w}{\partial r}+\frac{D}{r^2}\frac{\partial^2 w}{\partial r^2}-\frac{2\upsilon D}{r^4}\frac{\partial^2 w}{\partial\theta^2}\\
&-\frac{4(1-\upsilon)D}{r^3}\frac{\partial^3 w}{\partial r\partial\theta^2}-\frac{D}{r}\left(\frac{1}{r}+2(1-\upsilon)\right)\frac{\partial^4 w}{\partial r^2\partial\theta^2}+\left(e_0 a\right)^2\nabla^2\left(A+B\right)=B
\end{aligned}, \tag{34}$$

$$hh_{11}\left(\frac{\partial^2 u_0}{\partial r^2}+\frac{\partial^2 w_0}{\partial r^2}\frac{\partial w_0}{\partial r}\right)-2\in_{11}\left(\frac{\partial^2\varphi}{\partial r^2}\right)=0\,, \tag{35}$$

where

$$A=-\frac{1}{r}\left(k_{11}+k_{12}\right)\frac{\partial u}{\partial r}\frac{\partial w}{\partial r}-k_{11}\frac{\partial^2 u}{\partial r^2}\frac{\partial w}{\partial r}-k_{11}\frac{\partial u}{\partial r}\frac{\partial^2 w}{\partial r^2}-\frac{k_{11}}{2r}\left(\frac{\partial w}{\partial r}\right)^3-\frac{3}{2}k_{11}\left(\frac{\partial w}{\partial r}\right)^2\frac{\partial^2 w}{\partial r^2}$$
$$-\frac{k_{12}}{r}u\frac{\partial^2 w}{\partial r^2}-\frac{k_{12}}{r}\frac{\partial^2 v}{\partial r\partial\theta}\frac{\partial w}{\partial r}-\frac{k_{12}}{r}\frac{\partial v}{\partial\theta}\frac{\partial^2 w}{\partial r^2}-\frac{k_{12}}{r^3}\left(\frac{\partial w}{\partial\theta}\right)^2\frac{\partial w}{\partial r}-\frac{3k_{12}}{r^2}\frac{\partial^2 w}{\partial r\partial\theta}\frac{\partial w}{\partial\theta}\frac{\partial w}{\partial r}$$
$$-\frac{k_{12}}{r^2}\left(\frac{\partial w}{\partial\theta}\right)^2\frac{\partial^2 w}{\partial r^2}-\frac{h}{r}h_{11}\frac{\partial\varphi}{\partial r}\frac{\partial w}{\partial r}-hh_{11}\frac{\partial^2\varphi}{\partial r^2}\frac{\partial w}{\partial r}-hh_{11}\frac{\partial\varphi}{\partial r}\frac{\partial^2 w}{\partial r^2}-\frac{k_{12}}{r^2}\frac{\partial^2 u}{\partial r\partial\theta}\frac{\partial w}{\partial\theta} \tag{36}$$
$$-\frac{k_{12}}{r^2}\frac{\partial u}{\partial r}\frac{\partial^2 w}{\partial\theta^2}-\frac{k_{12}}{2r^2}\left(\frac{\partial w}{\partial r}\right)^2\frac{\partial^2 w}{\partial\theta^2}-\frac{k_{22}}{r^3}\frac{\partial u}{\partial\theta}\frac{\partial w}{\partial\theta}-\frac{k_{22}u}{r^3}\frac{\partial^2 w}{\partial\theta^2}-\frac{k_{22}}{r^3}\frac{\partial^2 v}{\partial\theta^2}\frac{\partial w}{\partial\theta}$$
$$-\frac{k_{22}}{r^3}\frac{\partial v}{\partial\theta}\frac{\partial^2 w}{\partial\theta^2}-\frac{3k_{22}}{r^4}\frac{\partial^2 w}{\partial\theta^2}\left(\frac{\partial w}{\partial\theta}\right)^2,$$

$$B=-hh_{11}\frac{\partial\phi}{\partial r}\frac{\partial w}{\partial r}+I_0\frac{\partial^2 w}{\partial t^2}-I_2\frac{\partial^2}{\partial t^2}\left[\frac{1}{r}\frac{\partial}{\partial r}\left(r\frac{\partial w}{\partial r}\right)+\frac{1}{r^2}\frac{\partial^2 w}{\partial\theta^2}\right]+K_{1w}w_0+K_{2w}w_0^3-G_p\nabla^2 w_0. \tag{37}$$

3 DQM

In the DQM, the derivatives of a function are approximated with weighted sums of the function values at a group of grid points. Therefore, set of PDEs are converted to set of algebraic equations. For implementation of the DQM approximation, consider a function $f(R,\theta)$ which has the field on a circular domain ($0\le\theta\le 2\pi$) with $n_r\times n_\theta$ grid points along r and θ axes. According to DQM, the r^{th} derivative of a function $f(R,\theta)$ can be defined as [12, 20]

$$\frac{\partial^n f_r\left(r_i,\theta_j\right)}{\partial r^n}=\sum_{k=1}^{N_r}A_{r,ik}f\left(r_k,\theta_j\right) \tag{38}$$

where C_{ij}^{ζ} are weighting coefficient and defined as:

$$A_{r,ij}=\begin{cases}\dfrac{M\left(r_i\right)}{\left(r_i-r_j\right)M\left(r_j\right)} & for \quad i\neq j \quad i,j=1,...,N_r\\ -\displaystyle\sum_{\substack{j=1\\ i\neq j}}^{N_r}A_{r,ij} & for \quad i=j \quad i,j=1,...,N_r\end{cases} \tag{39}$$

where $M(\zeta_i)$ is presented as:

$$M\left(r_i\right)=\prod_{j=1}^{N_r}\left(r_i-r_j\right) \tag{40}$$

The weighting coefficients for the second, third and fourth derivatives are defined as:

$$A_{ij}^{(2)}=\sum_{k=1}^{n_r}A_{ik}^{(1)}A_{kj}^{(1)},\quad A_{ij}^{(3)}=\sum_{k=1}^{n_r}A_{ik}^{(1)}A_{kj}^{(2)}=\sum_{k=1}^{n_r}A_{ik}^{(2)}A_{kj}^{(1)},\quad A_{ij}^{(4)}=\sum_{k=1}^{n_r}A_{ik}^{(1)}A_{kj}^{(3)}=\sum_{k=1}^{n_r}A_{ik}^{(3)}A_{kj}^{(1)}. \tag{41}$$

In a similar method, the weighting coefficients in θ-direction can be obtained. The coordinates of Chebyshev–Gauss–Lobatto grid points are chosen as:

$$\begin{aligned} r_i &= \frac{(R_0 - R_i)}{2}\left[1 - \cos\left(\frac{i-1}{N_r - 1}\right)\pi\right] \qquad i = 1,...,N_r \\ \theta_j &= \frac{(j-1)2\pi}{N_\theta - 1} \qquad j = 1,...,N_\theta \end{aligned} \tag{42}$$

where N_r and N_θ are number of grid points in radial and circumferential directions, respectively. Also, the clamped boundary condition in DQM form can be written as follows

$$\begin{cases} \bar{U}_{1j} = \bar{V}_{1j} = \bar{W}_{1j} = 0 \quad , \quad \sum_{k=1}^{N_r} A_{r,2k}\bar{W}_{kj} = 0 \\ \bar{U}_{N_r j} = \bar{V}_{N_r j} = \bar{W}_{N_r j} = 0 \quad , \quad \sum_{k=1}^{N_r} A_{r,(N_r-1)k}\bar{W}_{kj} = 0 \end{cases} \quad for\ j = 1,...,N_\theta \tag{43}$$

Applying DQM to Eqs. (32)-(35), yield the following matrix equation

$$\left(\left[\underbrace{K_L + K_{NL}}_{K}\right] + \Omega^2[M]\right)\begin{Bmatrix}\{Y_b\}\\ \{Y_d\}\end{Bmatrix} = 0 \tag{44}$$

where $[M]$ is the mass matrix, $[K_L]$ is the linear stiffness matrix, $[K_{NL}]$ is the nonlinear stiffness matrix and Ω is nonlinear frequency of the system. Also, $\{Y_b\}$ and $\{Y_d\}$ are boundary and domain points of the displacement which can be defined as:

$$\begin{cases} \{Y_b\} = \left\{\bar{U}_{1j}^{(x)T}, \bar{U}_{N_r j}^{(x)(x)}, \bar{V}_{1j}^{(x)T}, \bar{V}_{N_r j}^{(x)T}, \bar{W}_{1j}^{(x)T}, \bar{W}_{2j}^{(x)T}, \bar{W}_{(N_r-1)j}^{(x)\ T}, \bar{W}_{N_r j}^{(x)T}\right\}^T \\ j = 1,...,N_\theta \end{cases} \tag{45}$$

$$\begin{cases} \{Y_d\} = \left\{\bar{U}_{ij}^{(x)T}, \bar{V}_{ij}^{(x)T}, \bar{W}_{ij}^{(x)T}\right\}^T \\ \begin{cases} i = 3,...,N_r - 2 \\ j = 1,...,N_\theta \end{cases} \end{cases} \tag{46}$$

This nonlinear equation can now be solved using a direct iterative method to obtain the nonlinear frequency of the SLABNS.

4 NUMERICAL RESULTS AND DISCUSSION

The results presented here are based on the following data used for geometry and material properties of SLABNS [11, 16 and 21]:

$$a = 11.43\,nm, \quad b = 12.31\,nm, \quad h = 0.075\,nm,$$
$$\alpha_x = 1.2\times10^{-6}, \quad \alpha_\theta = 0.6\times10^{-6}, \quad E = 1.8\,Tpa, \quad \upsilon = 0.34,$$
$$h_{11} = 0.95\,C/m, \quad \rho_{BN} = 3.4870\,gr/cm^3, \quad G_P = 2.071273\,N/m,$$
$$K_{1w} = 8.9995035\times10^{17}\,N/m^3, \quad K_{2w} = 2.071273\,N/m^5.$$

In order to show the effects of nonlocal parameter, surrounding elastic medium and temperature change, the frequency reduction percent and nonlinear frequency ratio are defined as follows

$$FRP = \left(\frac{\Omega_{local} - \Omega_{nonlocal}}{\Omega_{local}}\right)\times100$$
$$NFR = \frac{Nonlinear\ \ frequency\ \left(\Omega_{nl}\right)}{Linear\ \ frequency\ \left(\Omega_{l}\right)}$$

In the absence of similar publications in the literature covering the same scope of the problem, one can not directly validate the results found here. However, the present work could be partially validated based on a simplified analysis suggested by Mohammadi et al. [12] on vibration of the annular graphene sheets. For this purpose, an annular graphene sheet with $E = 1.06$ TPa , $\nu = 0.33$, $\rho = 2300\ Kg/m^3$, $h = 0.34$ nm , $r_1 = 10\ nm$ is considered. Assuming CPT for vibration of the annular graphene sheet and ignoring the nonlinear elastic medium, electric field and electric displacement in Eqs. (3) and (4), the results obtained here are compared with those of [12]. The results are shown in Table 1. in which dimensionless frequency (i.e. $\Omega = \omega r_1^2\sqrt{\rho h / D_{11}}$) for different nonlocal parameters and two boundary conditions (i.e. simply support and clamped support) are shown. As can be seen, the results of the present work have a good agreement with the Refs. [12], indicating validation of the present study.

The convergence and accuracy of the DQM in evaluating the dimensionless nonlinear frequency of the SLABNS is shown in Table 2. for different nonlocal parameters. Fast rate of convergence of the method are quite evident and it is found that twelve DQM grid points can yield accurate results.

Table 1
Comparison of the present results with annular graphene sheets for the first natural frequency

Nonlocal parameter ($e_0a\ (nm)$)	Simply support		Clamped support	
	Mohammadi et al. [12]	Present work	Mohammadi et al. [12]	Present work
0	4.9345	4.9345	10.2158	10.2158
0.5	4.8997	4.8995	10.1283	10.1285
1	4.7979	4.7980	9.8784	9.8789
1.5	4.6409	4.64011	9.4999	9.5002
2	4.4455	4.4459	9.0348	9.0353

Table 2
Convergence behavior and accuracy of the dimensionless nonlinear frequency against the number of DQM grid points

Number of grid points (N_r)	Nonlocal parameter ($e_0a\ (nm)$)				
	0	0.5	1	1.5	2
5	1.6523	0.4140	0.1509	0.1437	0.0984
7	1.7469	0.5491	0.2249	0.2094	0.1136
9	1.8215	0.6202	0.3324	0.2419	0.1573
11	1.8618	0.6586	0.3573	0.2617	0.1731
12	1.8619	0.6588	0.3574	0.2618	0.1733

Fig. 2 illustrates the FRP versus the nonlocal parameter for four cases including:
Case1: linear vibration analysis of SLABNS
Case2: Nonlinear vibration analysis of SLABNS
Case3: linear vibration analysis of SLAGS
Case4: Nonlinear vibration analysis of SLAGS
As can be seen, the FRP increases with increasing μ. It means that with increasing μ, the frequency of the coupled system becomes lower. This is due to the fact that the increase of nonlocal parameter decreases the interaction force between SLABNS atoms, and that leads to a softer structure. It is also concluded that the FRP (or frequency) of SLABNS is lower (or higher) than SLAGS. It is due to the fact that SLABNSs are subjected to the electric field and thermo-mechanical loading while SLAGSs are subjected to thermo-mechanical loading only. On the other hand, the electric field in SLABNS can increase the frequency of the system. Hence, application of SLABNS in nanostructures based vibration analysis is better than SLAGS. Furthermore, the FRP of SLABNS and SLAGS in nonlinear vibration response is lower than linear one. It is due the fact that in nonlinear analyzing the accuracy of the obtained results is higher than linear one.

The effect of elastic medium on the FRP versus the nonlocal parameter of SLABNS, respectively is shown in Fig. 3. Three different cases of elastic medium are considered. Case 1, Case 2 and Case 3 depict the (i) without elastic medium (ii) with Winkler medium (iii) with Pasternak medium, respectively. As can be seen, the FRP (or frequency) increases (or decreases) with increasing nonlocal parameter. It can be observed that the FRP for Cases 1 and 3 is maximum and minimum, respectively. In the other words, the frequency of the system for the case of SLABNS embedded in elastic medium is higher than other cases. It is because considering elastic medium increases the stiffness of the system. It is also obvious that the FRP (or frequency) of the Case 3 is lower (or higher) than Case 2. It is due to the fact that in Winkler medium, a proportional interaction between pressure and deflection of SLABNS is assumed, which is carried out in the form of discrete and independent vertical springs. Where as, Pasternak medium considers not only the normal stresses but also the transverse shear deformation and continuity among the spring elements.

Fig. 4 demonstrates the influence of thermal gradient on the FRP with respect to the nonlocal parameter. It could be said however, that FRP increases slightly as thermal gradient is increased. This is perhaps because increasing thermal gradient decreases the structure stiffness. In addition, the effect of thermal gradient on the FRP becomes more prominent at higher nonlocal parameter. The effect of nonlocal parameter on the NFR versus maximum amplitude of the SLABNS is plotted in Fig. 5. As can be seen, NFR increase with increasing maximum amplitude. Furthermore, the NFR (or linear frequency) is increased (or decresed) with increasing nonlocal parameter. This is most likely due to the fact that the increase of nonlocal parameter decreases the interaction force between SLABNS atoms, and that leads to a softer structure. Fig. 6 shows the effect of elastic medium on the NFR as a function of the maximum amplitude. Three cases for elastic medium is considered the same as Fig. 3. Obviously, the effect of elastic medium type on the NFR is similar to FRP in Fig. 3. It is also found that the elastic medium effect of the NFR becomes more remarkable at higher maximum amplitude. The effect of temperature change on the NFR versus the maximum amplitude is depicted in Fig. 7. Increasing temperature change decreases the structure stiffness and that leads to increase (or decreases) of the NFR (or linear frequency). Moreover, the change rate of the NFR becomes more prominent with increasing maximum amplitude.

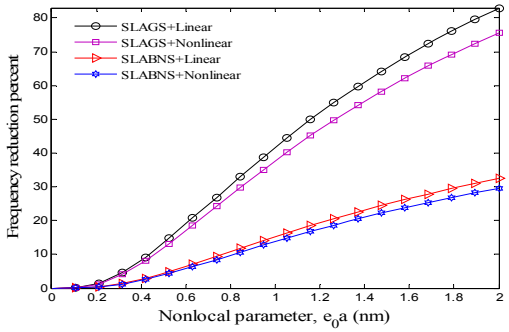

Fig. 2
FRP versus the nonlocal parameter for linear and nonlinear vibration of SLABNS and SLAGS.

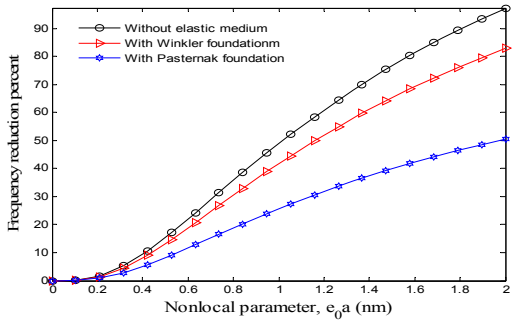

Fig. 3
The effect of elastic medium on the FRP versus the nonlocal parameter.

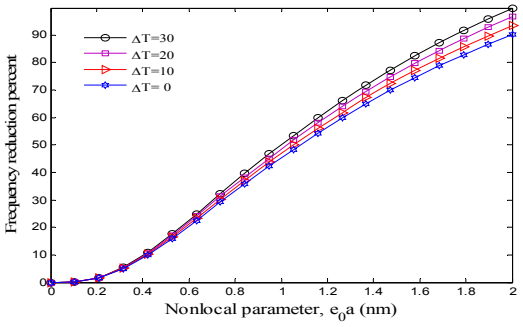

Fig. 4
The effect of thermal gradient on the FRP versus the nonlocal parameter.

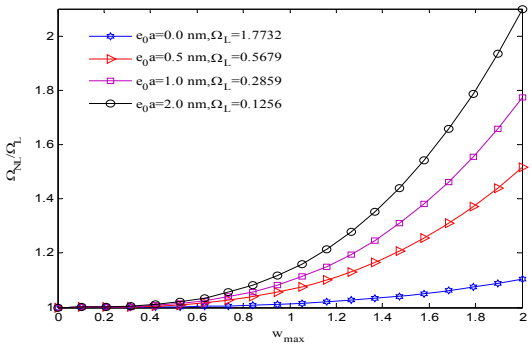

Fig. 5
The effect of nonlocal parameter on the NFR versus maximum amplitude.

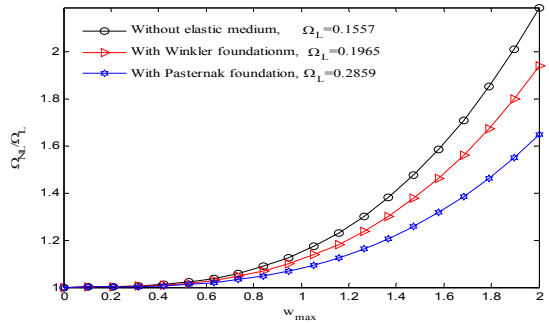

Fig. 6
The effect of elastic medium on the NFR versus maximum amplitude.

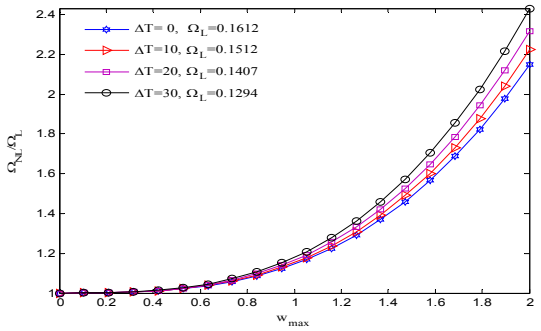

Fig. 7
The effect of temperature change on the NFR versus the maximum amplitude.

5 CONCLUSIONS

Based on nonlocal piezoelasticity theory, nonlinear vibration response of SLABNSs surrounded by Pasternak medium was investigated. Electro-thermo-mechanical coupled motion equations were solved using DQM in order to obtain the nonlinear frequency of the system. The effects of the nonlocal parameter, elastic medium, temperature change and maximum amplitude on the nonlinear frequency of the SLABNSs were taking into account. Numerical results show that the frequency of SLABNS was higher than SLAGS. It was also concluded that the FRP of SLABNS and SLAGS in nonlinear vibration response was lower than linear one. Furthermore, with increasing nonlocal parameter, the frequency of the coupled system becomes lower. In addition, considering elastic medium increases the stiffness of the system which leads to higher frequency. Moreover, increasing temperature change increases the NFR. The results of this study were validated as far as possible by Ref. [12]. This work was presented in order to design the SLABNSs based on nano-optomechanical and nano-electro-mechanical systems.

ACKNOWLEDGMENTS

The authors thank the referees for their valuable comments. The authors are grateful to University of Kashan for supporting this work by Grant No. 363443/8.

REFERENCES

[1] Salvetat J.P., Bonard J.M., Thomson N.H., Kulik A.J., Forro L., Benoit W., Zuppiroli L., 1999, Mechanical properties of carbon nanotubes, *Applied Physics A* **69**: 255-260.

[2] Baughman R.H., Zakhidov A.A., De Heer W.A., 2002, Carbon nanotubes--the route toward applications, *Science* **297**:787-792.

[3] Ma R., Golberg D., Bando Y., Sasaki T., 2004, Syntheses and properties of B–C–N and BN nanostructures, *The Royal Society* **362**: 2161-2186.

[4] Li Y., Dorozhkin P.S., Bando Y., Golberg D., 2005, Controllable modification of SiC nanowires encapsulated in BN nanotubes, *Advanced Materials* **17**:545-549.

[5] Behfar K., Naghdabadi R., 2005, Nanoscale vibrational analysis of a multi-layered graphene sheet embedded in an elastic medium, *Composite Science and Technology* **65**:1159-1164.

[6] Liew K.M., He X.Q., Kitipornchai S., 2006, Predicting nanovibration of multi-layered graphene sheets embedded in an elastic matrix, *Acta Materiala* **54**:4229-4236.

[7] Pradhan S.C., Phadikar J.K., 2009, Nonlocal elasticity theory for vibration of nanoplates, *Journal of Sound and Vibration* **325**:206-223.

[8] Shen L., Shen H.S., Zhang C.L., 2008, Nonlocal plate model for nonlinear vibration of single layer graphene sheets in thermal environments, *Computational Material Science* **48**:680-685.

[9] Ansari R., Rajabiehfard R., Arash B., 2010, Nonlocal finite element model for vibrations of embedded multi-layered graphene sheets, *Computational Material Science* **49**:831-838.

[10] Pradhan S.C., Kumar A., 2010, Vibration analysis of orthotropic graphene sheets embedded in Pasternak elastic medium using nonlocal elasticity theory and differential quadrature method, *Computational Material Science* **50**:239-245.

[11] Ghorbanpour Arani A., Kolahchi R., Mosallaie Barzoki A.A., Mozdianfard M.R., Noudeh Farahani S.M., 2012, Elastic foundation effect on nonlinear thermo-vibration of embedded double-layered orthotropic graphene sheets using differential quadrature method, *Proceeding of IMech Part C: Journal of Mechanical Engineering Science* **227**:1-8.

[12] Mohammadi M., Ghayour M., Farajpour A., 2012, Free transverse vibration analysis of circular and annular graphene sheets with various boundary conditions using the nonlocal continuum plate model, *Composite Part B: Engineering* **45**:32-42.

[13] Salehi-Khojin A., Jalili N., 2008, Buckling of boron nitride nanotube reinforced piezoelectric polymeric composites subject to combined electro-thermo-mechanical loadings, *Composite Science and Technology* **68**:1489-1501.

[14] Khodami Maraghi Z., Ghorbanpour Arani A., Kolahchi R., Amir S., Bagheri M.R., 2013, Nonlocal vibration and instability of embedded DWBNNT conveying viscose fluid, *Composites Part B: Engineering* **45**:423-432.

[15] Ghorbanpour Arani A., Kolahchi R., Vossough H., 2012, Nonlocal wave propagation in an embedded DWBNNT conveying fluid via strain gradient theory, *Physica B* **407**: 4281-4286.

[16] Ghorbanpour Arani A., Kolahchi R., Khoddami Maraghi Z., 2013, Nonlinear vibration and instability of embedded double-walled boron nitride nanotubes based on nonlocal cylindrical shell theory, *Applied Mathematical Modeling* **37**: 7685-7707.

[17] Ke L.L., Wang Y.S., Wang Z.D., 2012, Nonlinear vibration of the piezoelectric nanobeams based on the nonlocal theory, *Composite Structures* **94**:2038-2047.

[18] Ghorbanpour Arani A., Kolahchi R., Vossough H., 2012, Buckling analysis and smart control of SLGS using elastically coupled PVDF nanoplate based on the nonlocal Mindlin plate theory, *Physica B* **407**:4458-4465.

[19] Salajeghe S., Khadem S.E., Rasekh M., 2012, Nonlinear analysis of thermoelastic damping in axisymmetric vibration of micro circular thin-plate resonators, *Applied Mathematical Modeling* **36**:5991-6000.

[20] Malekzadeh P., Afsari A., Zahedinejad P., Bahadori R., 2010, Three-dimensional layerwise-finite element free vibration analysis of thick laminated annular plates on elastic foundation, *Applied Mathematical Modeling* **34**:776-790.

[21] Sepahi O., Forouzan M.R., Malekzadeh P., 2010, Large deflection analysis of thermo-mechanical loaded annular FGM plates on nonlinear elastic foundation via DQM, *Composite Structures* **92**: 2369-2378.